Proceedings of the Pakistan Academy of Sciences: A Physical and Computational Sciences 63(2): 133-146 (2026)

ISSN (Print): 2518-4245; ISSN (Online): 2518-4253
http://doi.org/10.53560/PPASA(63-2)717

Pakistan Academy of Sciences

Research Article

Homo- and Heteroleptic Cd(II) 4-Phenylbutyrates, Synthesis, Exploration of Chemistry, DNA Binding Study and Antileishmanial Activity

Aneeqa Sharif[1], Saba Naz[1], Saqib Ali[1*], Ali Haider[1], Sammar Yousuf[2,3], and Mahboob-ur-Rehman[4]

[1]Department of Chemistry, Quaid-i-Azam University, Islamabad, 45320, Pakistan
[2]H.E.J. Research Institute of Chemistry (International Center for Chemical and Biological Sciences) University of Karachi, Karachi-75270, Pakistan
[3]Institute of Molecular Biology and Biotechnology, University of Lahore, Lahore, Pakistan
[4]Department of Cardiology, Pakistan Institute of Medical Sciences (PIMS), Islamabad, Pakistan

Abstract: By using 4-phenylbutyric acid (4-PBA) and aromatic nitrogen heterocycles, i.e., 2,2′-bipyridine (BIPY), 1,10-phenanthroline (PHEN), and 2,9-dimethyl-1,10-phenanthroline (Me_2PHEN) as ancillary ligands, four cadmium carboxylates were synthesized. The chemistry and biological applications of the homoleptic complex are discussed for the 4-PB1, whereas the heteroleptic complexes containing BIPY, PHEN, and Me_2PHEN are designated as 4-PBB, 4-PBP, and 4-PBD, respectively. Their synthesis and chemistry were explored fully through FT-IR and NMR (^{1}H and ^{13}C) spectroscopy. The FT-IR data in the solid state show the metal coordination with the ligand moieties, where the carboxylate group adopted multi-mode coordination. The absence and presence of resonance signals, along with characteristic multiplicity in the solution ^{1}H as well as ^{13}C NMR data, confirm targeted synthesis. The assessment of the synthesized complexes for their binding ability with DNA was executed through multiple techniques, including UV-Vis absorption spectroscopy, viscometry, and cyclic voltammetry. The findings from all techniques support that the complexes interact with DNA through a dual mode of binding following a smooth process. The complex having an attached phenanthroline was found to be active in all attributed to its increased planar area and availability of bonding interactions. The antileishmanial study reveals that the synthesized complexes exhibit good to moderate activity against the amastigotes of *L. tropica* as compared to the standard drug used in the study.

Keywords: Homo- and Heteroleptic Carboxylates, Chelating Bidentate, Salmon Sperm DNA, Cyclic Voltammetry, *Leishmaniasis Tropica Promastigotes*, Gelardin's Strain.

1. INTRODUCTION

The burden of disease in terms of tropical and major non-communicable diseases is a big cause of hurdles for humans all over the world. The people belonging to the less developed countries are severely suffering from the neglected tropical disease, i.e., Leishmaniasis, also known as the disease of the poor. It is a parasitic infection caused by the bite of infected sandflies [1, 2]. On the other hand, cancer, the exact cause of which is still unknown, remains a big reason for mortality worldwide, affecting both developed and less developed countries alike. A prediction indicates that 16.3 million cases, which would be related to cancer and 29.5 million cases would be new by the time 2040 [3]. Despite global efforts by the healthcare sector to address this issue, the combined socioeconomic burden and adverse effects of currently in use drugs for cancer and leishmaniasis remain challenging. The fact

Received: April 2026; Revised: May 2026; Accepted: June 2026
* Corresponding Author: Saqib Ali <saqibali@qau.edu.pk>

that the well-known anti-cancer metallodrug cis-platin is active on account of its ability to interact with DNA motivates researchers in this direction [4]. The literature study reveals that DNA is the common target of the drugs used against cancer and many other communicable or non-communicable diseases [5].

There is a growing trend to modify the already in-use drug for the targeted response. The well-known example is the structural modification of the NSAIDs. This trend encourages the use of carboxylic acid as a ligand in the manufacture of metal-based therapeutics. The reason behind this is that the carboxylic acid is found to be an essential structural component of the majority of drugs. Besides this, the other structural and electronic characteristics of the carboxylic acids are well-suited for the biological system. Their ability to adopt a multi-coordination mode is considered important for getting interesting geometries that are well-matched to the biomacromolecules [6, 7]. The 4-phenylbutyric acid is an expectedly good choice in this regard, which already plays a significant biological role in plants by acting as a chemical binder [8]. It is prescribed to children to treat urea cycle disorder by scavenging ammonia, to cure inflammation, and mental disorders.

Being inspired by the biomacromolecule, the use of nitrogen heterocycles as auxiliary ligands alongside the carboxylic acid is a current research focus of scientists in the field of bioinorganic chemistry. The aromatic ring results in extended π systems, which could develop various non-covalent interactions [9]. This strategy results in a structure that could mimic the biomacromolecules and hence can compete and survive in the biological systems. The incorporation of the nitrogen heterocycle into the in-use drugs like furosemide and coumarin derivatives results in enhanced targeted results. Here, both the carboxylic acid and nitrogen heterocycles work together as primary and auxiliary ligands and result in fascinating topological and biological characteristics [10, 11]. Alongside this, the smart selection of the metal center matters a lot. Cadmium, a delicate, silvery-white metal with the atomic number 48 symbol Cd from Group 12, shares chemical similarities with zinc. It possesses fascinating chemistry and is capable of adopting various coordination geometries [12]. Cadmium can produce reactive oxygen species (ROS), alter mitochondrial potential and activate caspase enzymes, all of which combine to kill cancerous cells with minimal impact on healthy cells [13]. Additionally, recent research is investigating the use of quantum dots, targeted drug delivery, and nanoparticles based on cadmium [14]. Besides all this, the related toxicity is its weak point, which, however, could be compensated by complexation with suitable donor ligands, especially oxygen and nitrogen [15]. The Lewis acidity of the Cd(II) makes it quite useful in a number of catalytic processes. The coordination versatility makes it applicable in sensors. Its ability to adopt fascinating topological features results in the generation of structural frameworks when combined with suitable ligands and is used for the storage of gaseous or solid materials [16].

The study reveals that this kind of ligand and metal combination produces fascinating results in term of structure and application. The mixed ligand Cd(II) carboxylates derived from the substituted phenylacetic and nitrogen heterocycles show enhance binding with DNA as compare to relevant ligand and homoleptic carboxylates [15]. The coordination flexibility of the cadmium(II) and carboxylate group together with the nitrogen heterocycles leads to interesting and stable topological arrangements known “Chinese lantern” [17]. Similarly, 1D and 2D polymeric structural framework was observed for Cd(II) complexes as a consequence of coordination of nitrogen donor ancillary ligands and show interesting application as sensors [18]. The Cd(II) based mixed ligand carboxylates derived from the cyclic carboxylic acids show efficient ability to bind with DNA [19]. Taking into consideration the significant role of carboxylic acid and nitrogen heterocycles as ancillary ligands to modify the structure and hence applications, herein, homo- and heteroleptic carboxylates were synthesized. Their synthesis in pure form, followed by complete spectroscopic characterization, was carried out. Their DNA-binding ability was assessed through multiple techniques. They were also tested for their ability to act as an antileishmanial agent.

2. MATERIALS AND METHODS

The chemicals used during synthesis are 4-phenylbutyric acid, sodium bicarbonate, cadmium(II) nitrate, 2,2′-bipyridine,

1,10-phenanthroline, and 2,9-dimethyl-1,10-phenanthroline shown in Scheme 1. These chemicals were acquired from Aldrich, Fluka and Alfa-Aesar (Johnson Matthey); They were analytical grade and utilized as supplied without further purification. The solvents, i.e., methanol, ethanol, chloroform, acetone, and dimethyl sulphoxide (DMSO), were of analytical grade and obtained from Germany's Merck. The Gallenkamp electrothermal apparatus was used to determine melting points, which is manufactured in the UK. For the samples in solid state, the FT-IR data were recorded using a Bruker TENSOR II (Germany) spectrophotometer in the 4000–400 cm^{-1} range. The NMR (^{1}H and ^{13}C) behavior was investigated using a 300 MHz Bruker Advanced Digital NMR instrument. The electronic spectra were recorded using the Shimadzu 1800 UV-Visible spectrophotometer. A Corrtest CS 300 (Potentiostat/Galvanostat) Electrochemical Workstation, manufactured in China, was used to collect the record of the voltammograms.

2.1. Synthesis

2.1.1. Synthesis of sodium salt of ligand acid

The sodium bicarbonate aqueous solution (3 mmol, 0.252 g) was added gradually to the methanolic solution of 4-phenylbutyric acid (3 mmol, 0.498 g). The solution was continuously agitated at room temperature to prepare sodium salts of the respective acid. Stirring was continuous until neutralization. The solid product was obtained by evaporating the solvents under low pressure. The synthesis route is shown in Scheme 2.

2.1.2. Synthesis of homoleptic complex (4-PB1)

The synthesis route for 4-PB1 is shown in Scheme 3. Methanolic solutions of ligand sodium salt, 4-PBNa (3 mmol, 0.558 g), were added to an aqueous solution of Cd(II) nitrate (1.5 mmol, 0.355 g) and stirred continuously for seven to eight hours at 50 °C. The reaction mixtures were filtered off, and the solvent was evaporated using a rotary evaporator to obtain the solid products.

$[Cd(4\text{-}PBA)_2]$ (4-PB1)
Yield = 67%; Physical state: white powder solid; M.P. = 250-253 °C; FT-IR (4000–400 cm^{-1}): 1546 (COO^-_{asymm}); 1398 (COO^-_{symm}), 148 (Δν), 462 (Cd-O); ^{1}H NMR (in DMSO): 2.10-2.15 (t, 4H, H2, J = 7.5 Hz), 1.73-1.83 (quint, 4H, H3, J = 7.2 Hz), 2.49-2.61 (m, 4H, H4), 7.13-7.29 m (m, 10H, H6, 6′, H7,7′, H8); ^{13}C NMR (in DMSO): 180.3 (C1), 35.3 (C2), 28.4 (C3), 34.6 (C4), 142.6 (C5), 128.8 (C6, 6′), 128.6 (C7, 7′), 126.0 (C8).

2.1.3. Synthesis of heteroleptic complexes (4-PBB, 4-PBP, and 4-PBD)

Heteroleptic carboxylates synthesis was done using the same method as 4-PB1. The only exception was that 1.5 mmol ethanolic solutions of 2,2'-bipyridine, 1,10-phenanthroline, and 2,9-dimethyl-1,10-phenanthroline were added during continuous stirring at 50 °C along with cadmium (II) nitrate to synthesize 4-PBB, 4-PBP, and 4-PBD, respectively. After filtering the resultant solutions and using rotary evaporation to eliminate excess solvents, the solid products were repeatedly cleaned with water

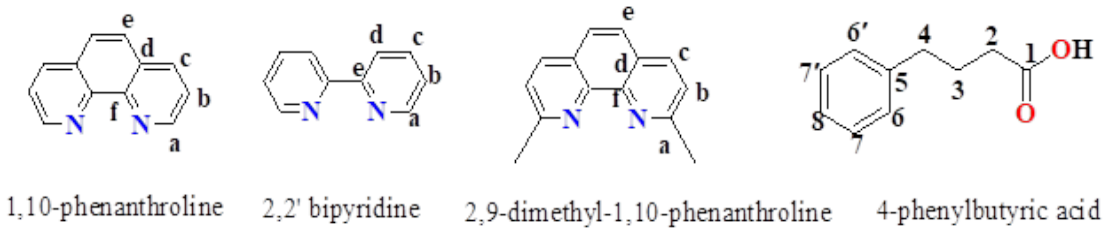

Scheme 1: Ligands structures used in synthesis, numbered for NMR analysis.

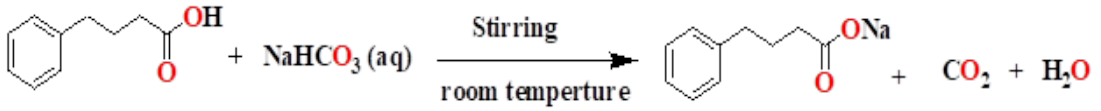

Scheme 2: Synthetic route for the sodium salt of 4-phenylbutyric acid (4-PBNa).

and allowed to air dry. The resulting compounds were recrystallized using a mixture of suitable solvents. All of the synthesized complexes' melting points were noted. Scheme 3 shows the synthesis pathway for complexes.

[Cd(4-PBA)$_2$(BIPY)] (4-PBB)

Yield = 73%; Physical state: white crystalline solid; M.P. = 123-125 °C; FT-IR (4000–400 cm^{-1}): 1550 (COO^-_{asymm}); 1407 (COO^-_{symm}), 143 (Δν), 420 (Cd-O), 533 (Cd-N), 763 $(C\text{-}H)_{out\ of\ plane}$; ^{1}H NMR (in $CDCl_3$): 2.31-2.36 (t, 2H, H2, J = 7.2 Hz), 1.85-1.95 (quint, 2H, H3, J = 8.1 Hz), 2.53-2.58 (t, 2H, H4, J = 7.5 Hz), 7.19-7.28 (m, 2H, H6, 6′), 7.09-7.16 (m, 3H, H7,7′, H8) ,8.92-8.94 (m, 1H,Ha), 7.48-7.53 (m, 1H, Hb), 7.94-7.99 (td, 1H, Hc, J = 1.8, 7.8 Hz), 8.12-8.14 (d, 1H, Hd, J=8.1); ^{13}C NMR (in $CDCl_3$): 182.6 (C1), 35.6 (C2), 28.1 (C3), 35.0 (C4), 128.5 (C5), 128.1 (C6, 6′), 126.1 (C7, 7′), 121.4 (C8), 149.6 (Ca), 125.5 (Cb), 139.6 (Cc), 142.3 (Cd), 150.5 (Ce).

[Cd(4-PBA)$_2$(PHEN)] (4-PBP)

Yield = 85%; Physical state: white crystalline solid; M.P. = 179-180 °C; FT-IR (4000–400 cm^{-1}): 1554 (COO^-_{asymm}); 1409 (COO^-_{symm}), 145 (Δν), 427 (Cd-O), 566 (Cd-N), 849, 728 $(C\text{-}H)_{out\ of\ plane}$; ^{1}H NMR (in $CDCl_3$): 2.49-2.57 (m, 6H, H2, H8), 1.85-1.93 (quintet, 4H, H3, J = 8.1 Hz), 2.30-2.36 (t, 4H, H4, J = 7.2 Hz), 7.07-7.21 (m, 10H, H6,6′, H7,7′), 9.11-9.14 (dd, 2H, Ha, J = 7.8, 1.8), 7.71-7.75 (m, 2H, Hb), 8.39-8.42 (dd, 2H, Hc, J = 1.5, 8.1Hz), 7.90 (s, 2H, He′); ^{13}C NMR (in $CDCl_3$): 182.4 (C1), 35.6 (C2), 28.2 (C3), 35.2 (C4), 128.4 (C5), 128.1 (C6, 6′), 125.5 (C7, 7′), 124.8 (C8), 150.4 (Ca), 126.9 (Cb), 141.2 (Cc), 138.6 (Cd), 129.0 (Ce), 142.3 (Cf).

[Cd(4-PBA)$_2$(Me$_2$PHEN)] (4-PBD)

Yield = 83%; Physical state: brown crystalline solid; M.P. = 156-158 °C; FT-IR (4000–400 cm^{-1}): 1548 (COO^-_{asymm}), 1410 (COO^-_{symm}), 138 (Δν), 418 (Cd-O); 550 (Cd-N), 859, 731 $(C\text{-}H)_{out\ of\ plane}$; ^{1}H NMR (in $CDCl_3$): 2.37-2.42 (t, 4H, H2, J = 7.2 Hz), 1.93-2.03 (quint, 4H, H3, J = 8.1 Hz), 2.60-2.66 (t, 4H, H4, J = 7.5 Hz), 7.10-7.28 (m, 10H, H6,6′, H7,7′, H8), 7.70-7.72 (d, 1H, Hb, J = 8.4 Hz), 8.33-8.36 (d, 2H, Hc, J = 8.1 Hz), 7.84 (s, 2H, He), 3.19 (s, 6H, H_{Methyl}); ^{13}C NMR (in $CDCl_3$): 182.7 (C1), 35.7 (C2), 28.3 (C3), 34.6 (C4), 128.1 (C5), 127.3 (C6, 6′), 126.1 (C7, 7′), 125.5 (C8), 161.2 (Ca), 125.9 (Cb), 140.6 (Cc,), 139.0 (Cd), 128.5 (Ce), 142.3 (Cf), 25.5 (C_{Methyl}).

2.2. DNA Binding Behavior through UV-Visible Spectroscopy

In 100 milliliters of deionized water, 20 milligrams of lyophilized powder of sodium salt of salmon

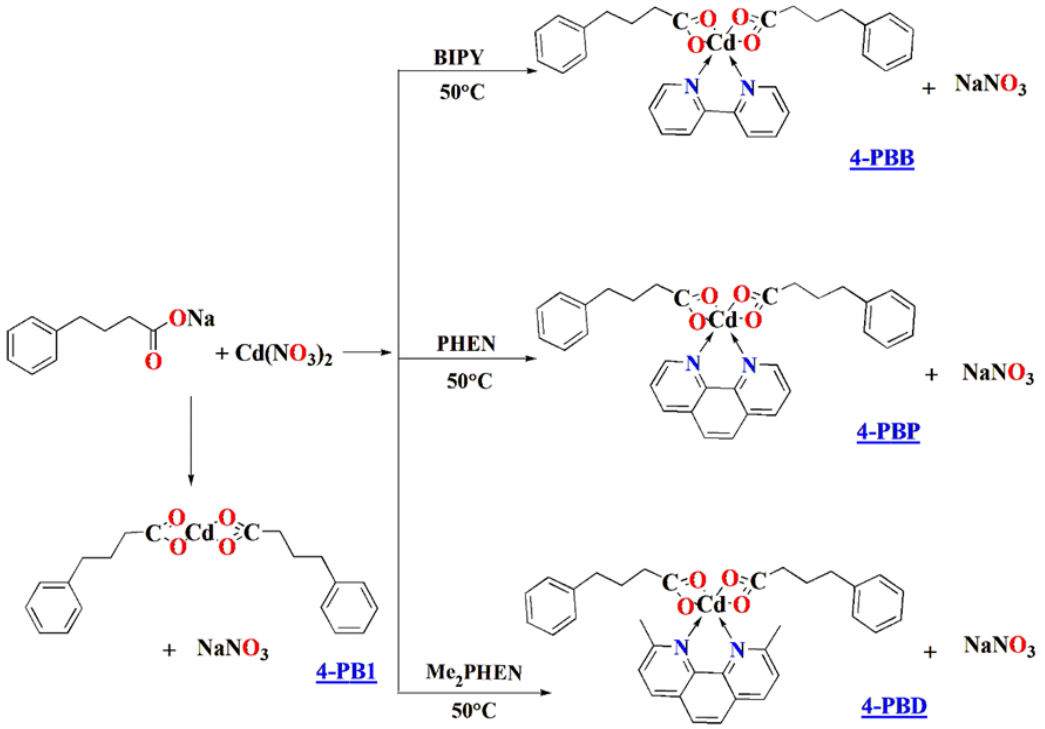

Scheme 3: Synthetic routes for complexes 4-PB1, 4-PBB, 4-PBP, and 4-PBD.

sperm were dissolved for roughly 24 hours while being continuously stirred. The DNA sample was found to be pure, with an absorption ratio (260/280) of 1.68, corresponding to a DNA concentration of 166 μM. Ethanol was used as a solvent for the ligand 4-PBA and relevant complexes 4-PB1, 4-PBB, 4-PBP, and 4-PBD. The absorption spectra were recorded at different DNA concentrations, with the ligand and complexes at a fixed concentration. To counteract the DNA absorption effect, the reference and sample cells were having same amount of DNA throughout the experiments. The compound-DNA solution was incubated for roughly ten minutes following each addition, then the spectra were recorded [20].

2.3. DNA Binding Behavior through Cyclic Voltammetry

Using 0.1M TBAP (tetrabutyl ammonium perchlorate) as the supporting electrolyte, the electrochemical process of the ligand acid 4-PBA and its corresponding complexes (4-PB1, 4-PBB, 4-PBP, and 4-PBD) in DMSO solutions was investigated. Measurement was taken on a Corrtest CS 300 (Potentiostat/Galvanostat) Electrochemical Workstation manufactured in China. The working electrode, counter electrode, and reference electrode in this three-electrode electrochemical workstation are glassy carbon having a surface area of 0.03 cm^2, platinum wire, and saturated silver/silver chloride (Ag/AgCl), respectively. The GC electrode was polished and cleaned by an aqueous slurry of alumina (Al_2O_3) using a nylon buffing pad. The experiments were conducted at room temperature in the presence of Ar gas, both with and without varying amounts of SS-DNA [21].

2.4. DNA Binding Behavior through Viscometry

Viscometry was also used to investigate the compound-DNA interaction by using an Oswald viscometer. The time required for the flow of the DNA solution was measured using a digital stopwatch both as the compounds were added gradually and on their own. The average flow time was determined after the experiment was run three times. η° was calculated by using the flow times of the pure solvent and the DNA solution. The η was computed as the difference among the flow times of pure standard DNA solution (t) and DNA solution with different complex concentrations (t°). The viscosities of the DNA solution alone and having varying concentrations of ligand and derived complexes were then plotted on the graph between $(\eta/\eta°)^{1/3}$ and [Compound]/[DNA] [22].

2.5. Antileishmanial Activity

Anti-leishmanial screening against two strains of *Leishmania,* i.e., *L. tropica* (promastigotes), of all synthesized co-crystals 2-7. RPMI 1640 media (Sigma, ST. Louis, USA) containing 10% fetal bovine serum (PAA Lab GmbH, Australia) was used to cultivate leishmanial parasites. The analysis was conducted using Leishmania culture at a density of 1×10^6 cells/mL. The experiment was carried out in a Costar 96-well plate with concentrations ranging from 1 mg/mL to six serial dilutions. Leishmanial cells at a concentration of 1×10^6 were utilized as the control and RPMI medium as the blank. A Cooled incubator was used to incubate the seeded 96-well plate with test dilutions for 72 hours. Using an inverted microscope, the culture was examined for cell viability. The MTT assay was performed the OD was measured at 540 nm. The program EZ-Fit 5.03 Perrella Scientific was used to get the IC_{50} values [23]; furthermore, similar values of IC_{50} were observed in a previous study by Ebrahimisadr *et al*., [24].

3. RESULTS AND DISCUSSION

The four targeted complexes were synthesized in good acceptable yield and pure condition, which is clear from their short-range melting points. They exhibit solubility in DMSO, chloroform, ethanol, and acetone, etc. The physical data is presented in Table S1, whereas the relevant spectroscopic characterization and the activities, which include DNA binding studies and antileishmanial ability, are discussed in the following sections**.**

3.1. FT-IR Spectroscopic Studies

The solid-state FT-IR data recorded in 400 to 4000 cm^{-1} are presented in Table S2, whereas the selected data are also present in the experimental section**.** The acid deprotonation is verified by the lack of a prominent band at 3500-3000 cm^{-1} as a result of the hydroxyl (-OH) group of the acid. The complexation is apparent by the formation of new bands between 400 to 550 cm^{-1} due to Cd-O/N bonds. The bands associated with C=O at

1685 cm^{-1} were replaced with two new vibrational bands. One indicated COO^- asymmetric (1554–1546 cm^{-1}) and the other COO^- symmetric (1410–1398 cm^{-1}) vibrations provided a clue for the complex formation. [25, 26]. Their difference., $\Delta\upsilon = COO_{asymm}$- COO_{symm} is of significant importance to get a clue about the possible coordination mode adopted by the carboxylate moiety [27, 28]. Deacon and Phillips, studied a large number of FT-IR data of acetates and concluded that $\Delta\upsilon < 200$ cm^{-1} indicated the presence of bidentate coordination, while a monodentate mode is indicated by $\Delta v > 200$ cm^{-1}. Another difference between bidentate (i.e., chelating) and bridging is that the former has a smaller $\Delta\upsilon$ [29]. According to this description, a chelating bidentate mode of coordination, with $\Delta\upsilon$ values of 178 cm^{-1}, 156, 145, and 134, is expected for complexes 4-PB1, 4-PBB, 4-PBP, and 4-PBD, respectively. Two new significant bands in the fingerprint region appear in the 400–600 cm^{-1} range, confirming the coordination of the N-donor moiety and acid ligand to the metal center [30]. Strong vibrational bands in the region 700–900 cm^{-1}, which correspond to C–H out-of-plane vibrations from the aromatic nitrogen heterocyclic ligands, were seen in all of the heteroleptic Cd complexes. These observed vibrational bands are similar to those reported previously [31]. The C-H (out of plane) vibrational bands for the heterocyclic aromatic rings at 774 cm^{-1} (BIPY in 4-PBB), 726 cm^{-1} (PHEN in 4-PBP), and 734 cm^{-1} (Me_2PHEN in 4-PBD) verified the binding of BIPY, PHEN, and Me_2PHEN in complexes. These are in accordance with the observed FT-IR data of the reported similar complexes [32, 33].

3.2. Multi-Nuclear NMR (^{1}H, ^{13}C) Spectroscopy

3.2.1. ^{1}H NMR spectral description

The loss of the hydroxyl proton signal in the synthesized carboxylates' NMR spectrum is a clear indication that the ligand acids were deprotonated. The other protons of the ligand moieties are only slightly shifted in their corresponding spectrum areas, suggesting that they are not directly involved in coordination with the metals [8, 34]. The existence of the N-donor heterocycle in the structure of the synthesized complexes is indicated by signals in the less shielded part of the spectra that indicates the downfield region of the spectra. Complex (4-PBB), containing 2,2'-bipyridine as a nitrogen-donor heterocycle, exhibits spectra with four extra signals arising from the four protons of the heterocycle in a distinctive multiplicity pattern. These protons' chemical shift values were given in the following sequence: Ha > Hd > Hg > Hb, which is in accordance with their free precursor and published data for analogous complexes Complexation of the 1,10-phenanthroline is indicated by the four extra signals seen in the spectra of 4-PBP, which were given chemical shift values in the following order: Ha > Hg > He > Hb. These values fall within the range reported for Phen-based complexes [35]. The presence of 2,9-dimethyl-1,10-phenanthroline is verified by the three new signals present in the deshielded part of 4-PBD spectra, which are resonating signals as well as the singlet at 3.19 ppm ascribed to the methyl group proton. They were given chemical shift values that correspond to the free Me_2Phen ligand in the following order: Hg > He > Hb. The magnetic anisotropic effect, along with the electric dipoles connected to the N-atom, causes these peaks to move to the lower field [36]. The ^{1}H NMR spectra of all complexes are presented in the supplementary file in Figures S1 to S4.

3.2.2. ^{13}C NMR spectral description

^{13}C NMR spectroscopy, which detected the resonance signals from each carbon of the ligand moiety and the nitrogen donor heterocycles, provided additional support for the findings of the ^{1}H NMR spectral analysis. The spectra of the related complexes show a considerable downfield shift at 178.3 ppm for the resonance signal attributed to the C=O group of the ligand 4-PBA. This downfield shift is explained by the deprotonated carboxylate group working in combination with the positively charged metal center to remove this group's electron density. Five extra signals arise in the spectra of complexes 4-PBB, showing attachment of the bipyridine. Its carbon exhibits resonance, and the order of its chemical shift values is Ce > Ca > Cd > Cg > Cb [3]. The emergence of six new signals indicates the coordination of 1,10-phenanthroline and 2,9-dimethyl-1,10-phenanthroline in the spectra of complexes 4-PBP and 4-PBD. These signals have been assigned chemical shift values in the following order: According to the free precursors and their related reported complexes, Ca > Cz > Cg > Cd > Ce > Cb [19]. The ^{13}C NMR spectra of all complexes are presented in the supplementary file in Figure S1 to S4.

3.3. DNA Binding Behavior using UV-Visible Spectroscopy

Using UV-Visible spectroscopy, the ability of the ligand 4-phenylbutyric acid (4-PBA) and its complexes to interact with DNA was examined. The absorption spectra of all the complexes with and without DNA addition are presented in Figure 1. Absorption values within 230 and 320 nm were ascribed to intra-ligand π–π* transitions in the absence of DNA [38]. The method of interaction is typically shown by the spectra obtained by following a consecutive addition of DNA. Ligand (4-PBA) exhibits a hypochromic effect without any accompanying shift in absorption maxima. Some authors in previous studies describe that such changes are associated with groove binding and others with the intercalation. This data has been presented previously, and an intercalative binding interaction is described for the said ligand in the cited data [8].

The absorption spectra of the complexes presented in Figure 1 clearly reveal that the incremental addition of DNA causes a decrease in the absorption intensity, i.e., a hypochromic effect. This hypochromism is the result of a decrease in the electronic transition. The orbital of the DNA and the respective interacting moieties overlap during interaction. The empty or partially filled orbital gets filled, leading to a hypochromic effect. This is accompanied by a red shift for the complex 4-PB1, indicating that the said complex interacts with DNA through intercalation [39]. The spectra of other complexes, as presented in Figure 1, reveal a red to no shift in their absorption maxima.

Loganathan *et al*. [40] favored groove binding above intercalation for such kinds of changes, while Mishra *et al*. [41] observed that the presence of hypochromic effect instead of any corresponding wavelength shift is considered the outcome of intercalation. This leads to the conclusion that they interact with DNA through a dual way of binding, i.e., groove and intercalation [42].

The binding constant (Kb) values were measured using the Benesi-Hildebrand equation,

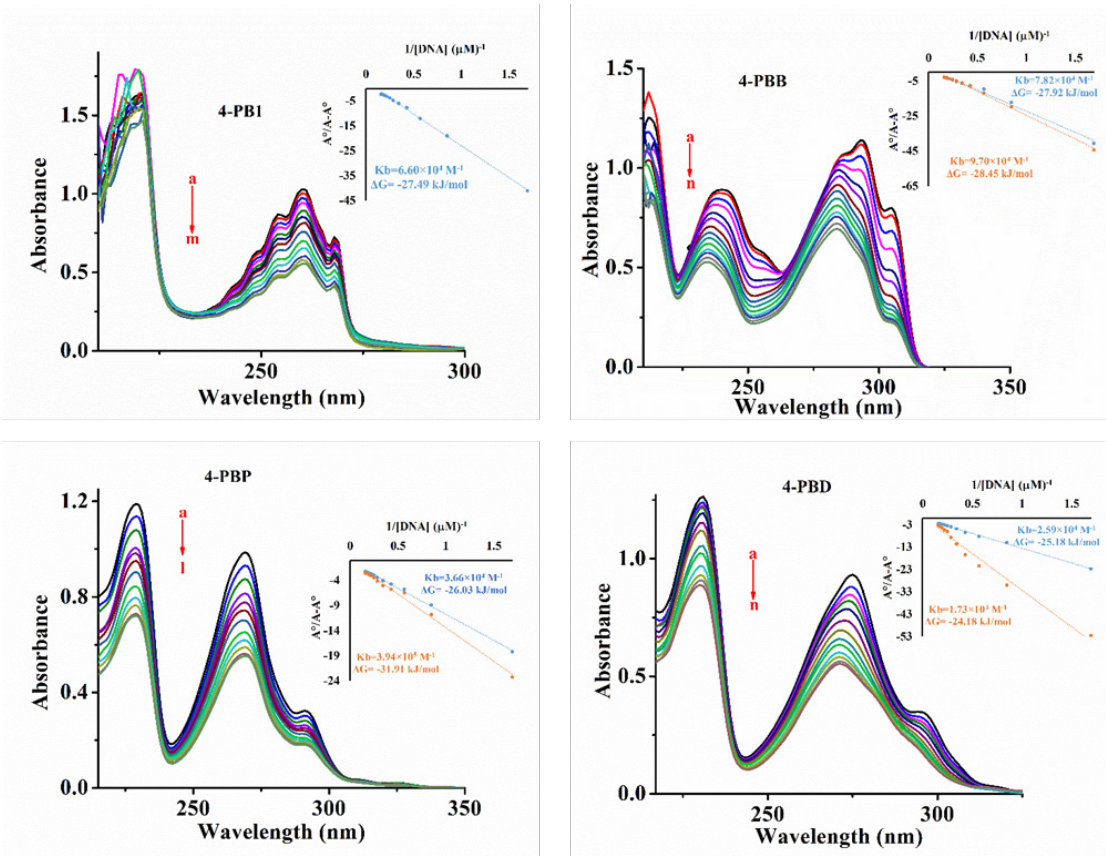

Fig. 1. Absorption spectra of the complexes recorded in the absence and in the presence of increasing DNA concentrations (0.74–7.11 μM for 4-PB1, 0.74–7.67 μM for 4-PBB, 0.74–5.77 μM for 4-PBP, and 0.74–7.67 μM for 4-PBD). In each spectrum, line (a) indicates the free complex, while the remaining lettered spectra represent progressively increasing DNA concentrations.

which is given in the cited data along with its figurative explanation. Using this, the plot was plotted between $A^{\circ}/A\text{-}A^{\circ}$ as ordinate and 1/[DNA] as abscissa. The ratio of intercept to slope (c/m) was calculated, which gives the value of Kb, i.e., the efficiency of binding (see Table 1) [43]. The complexes have higher Kb values than the ligands, attributed to the chelating action. This enhances the complexes' planner activity and functioning and enables effective stacking between DNA base pairs, resulting in increased binding [44]. The complex 4-PBP with phenanthroline attached as the heterocycle moiety exhibited the strongest binding. This is probably because of the expanded planar area of the strong intercalating 1,10-phenanthroline, chelation, and π-π* interaction. This kind of behaviour has been observed for the reported phenanthroline based complexes [45]. The Gibbs free energy was calculated to get an understanding of the process's viability, i.e., whether it was feasible or not:

$$\Delta G = -RT \ln Kb$$

As previously reported for comparable complexes, the data for this parameter show that the ligand acids and their complexes undergo a spontaneous binding process [39].

3.4. DNA Binding Behavior using Cyclic Voltammetry (CV)

The cyclic voltammetry-based DNA-interaction studies reinforced the results of the UV-visible absorption spectroscopy. The electrochemical data (CV) were recorded during a gradual increment in DNA concentration. The changes in the cyclic voltammograms were observed to decide about the manner in which DNA binding proceeds. Compounds with more than one redox center often show peaks or formal potentials that are both positive and negative at the same time, and increases or decreases in current intensity. Findings from the literature indicate that a positive shift is indicative of an intercalative mode of binding, whereas a positive shift mixed with a negative shift shows dual interaction [41]. The complexes' voltammograms are presented in Figure 2. The voltammogram of ligand 4-PBA is reported in the cited data [8]. The complex 4-PB1 experienced a positive shift in the relevant oxidation and reduction peaks, indicating its interaction with DNA through intercalation (see Figure 2). The oxidation and reduction potential peaks of aromatic heterocycles and redox couples linked to the structural motifs of synthesized complexes 4-PBB, 4-PBP, and 4-PBD exhibit a heterogeneous pattern of change (see Table S2). For complexes involving many oxidation-reduction potentials, the combination of these changes in the complexes' voltammograms is very typical [46]. It's crucial to remember that the complex 4-PBB's cyclic voltammogram showed one separate oxidation and reduction, which was linked to the emergence of new potential electroactive species. Because the concentration of the electroactive species decreases and the attached species diffuses slowly towards the electrode surface, the complex binding to the DNA causes a drop in current [47]. On the other hand, the species that become adsorbed on the electrode's surface could be the cause of the perceived rise in current intensity, offsetting the actual decrease in current [48].

3.5. DNA binding behaviour using Viscometry

DNA binding can also be studied through viscometry

Table 1. Binding constant (Kb) and Gibbs' free energy (ΔG) against the respective λmax.

Codes	Compound	λ_{max} (nm)		Kb (M^{-1})	ΔG (KJ/mol)
		Before DNA	After DNA		
4-PB1	$[Cd(4\text{-}PBA)_2]$	260	260	6.60×10^4	-27.49
4-PBB	$[Cd(4\text{-}PBA)_2BIPY]$	286	283	9.70×10^4	-28.45
		240	234	7.82×10^4	-27.92
4-PBP	$[Cd(4\text{-}PBA)_2PHEN]$	269	-	3.66×10^5	-31.73
		229	-	3.94×10^5	-31.91
4-PBD	$[Cd(4\text{-}PBA)_2(Me_2PHEN)]$	274	271	2.59×10^5	-30.88
		230	229	1.73×10^5	-29.88

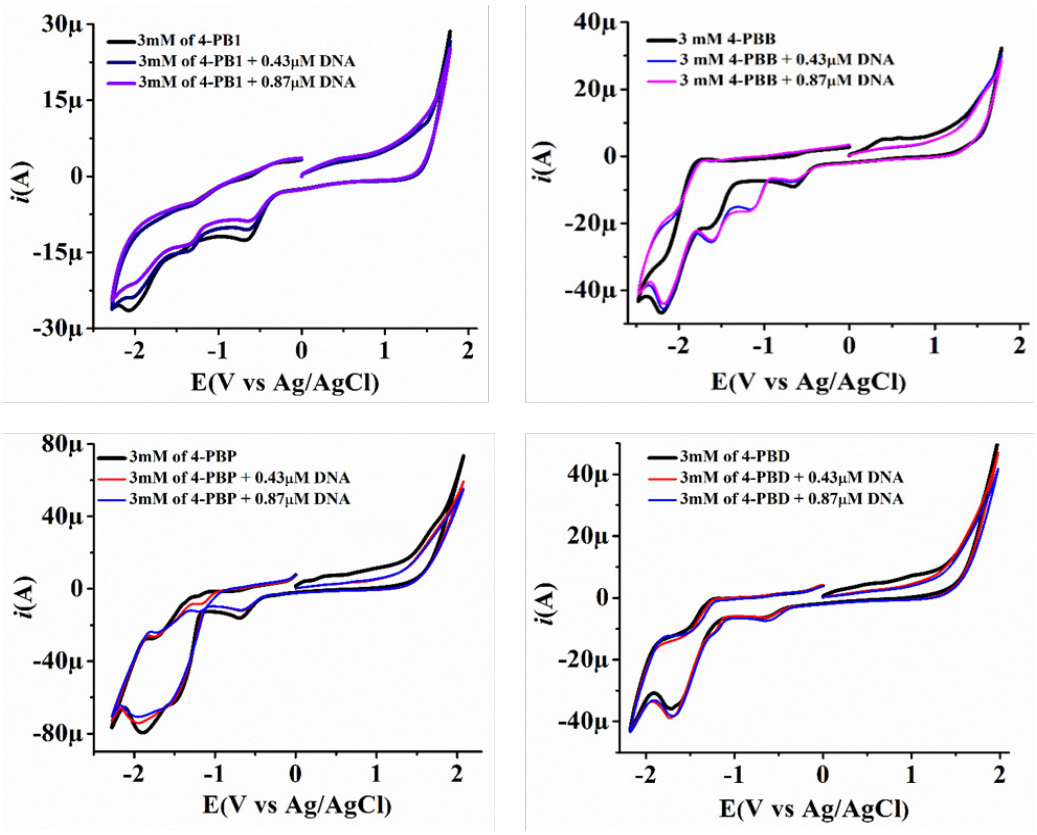

Fig. 2. Cyclic voltammograms of the complexes in the absence and during increasing concentration of DNA.

and the test which is significant to indicate this binding is the hydrodynamic measurements because they are sensitive to variations in length. A literature review shows that an increase in viscosity values is the outcome of DNA interaction via the intercalation mode. This is due to the DNA base pairs' lengthening to make room for the binding moieties. Conversely, non-intercalative interactions occur in the DNA helical structure folding or bending, which causes the viscosity to drop little or not at all [49]. Figure 3 makes it clear how the ligand acid 4-PBA interaction behaviour and its complexes affect the viscosity of DNA. In the case of ligand acid 4-PBA and complex 4-PB1, a consistent rise in viscosity was noted, which is suggestive of the intercalation method. On the other hand, all other complexes exhibit a moderate to gradual increase/ irregularity that enables the coexistence of surface binding modes and intercalation.

3.6. Antileishmanial Activity

The antileishmanial effectiveness of the ligand 4-PBA and its homo- and heteroleptic cadmium (II) carboxylates against *Leishmania tropica* promastigotes was evaluated using the ATCC strain. Promastigote vitality was evaluated in both treated and control samples after a 24-hour incubation period. Surprisingly, treated samples showed a significant decrease in viability when compared to control samples, as shown in Table 2. The ligand 4-PBA appeared to be inactive against tested standards with IC_{50} values of 3.39 ± 0.01,

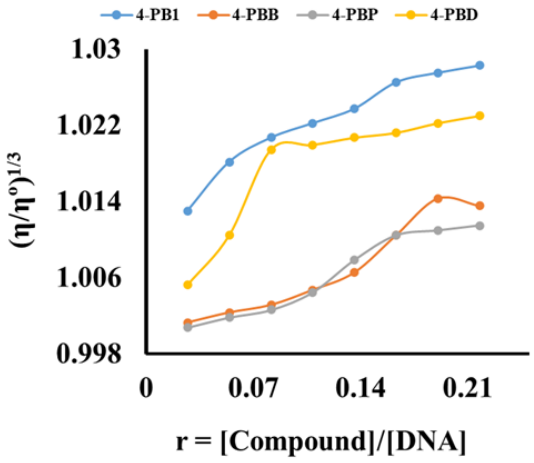

Fig. 3. Graph indicating the effect of a change in the viscosity of DNA.

Table 2. Antileishmanial activity (IC_{50} ± S.D.) of ligand and synthesized Cd(II) carboxylates.

Code	Sample	IC_{50} (μM) ± S.D.
4-PBA	4-Phenylbutyric acid	60.35 ± 0.02
4-PB1	$[Cd(L1)_2]$	40.35 ± 0.02
4-PBB	$[Cd(L1)_2bipy]$	24.54 ± 0.02
4-PBP	$[Cd(L1)_2Phen]$	15.63 ± 0.05
4-PBD	$[Cd(L1)_2(Me_2Phen]$	18.16 ± 0.02
Standard Drugs	Amphotericin	3.39 ± 0.01
	Miltefosine	31.8 ± 0.02
	Pentamidine	9.23 ± 0.01

31.8 ± 0.02, and 9.23 ± 0.01 μM for amphotericin, miltefosine, and pentamidine, respectively [50]. However, all synthesized cadmium metal complexes showed good to moderate anti-leishmanial potential against *L. tropica*. Among them, $[Cd(L1)_2Phen]$ (4-PBP, IC_{50} = 15.63 ± 0.05 μM) appeared to be the most potent antileishmanial agent, followed by $[Cd(L1)_2(Me_2Phen]$ (4-PBD, IC_{50} = 18.16 ± 0.02 μM) and $[Cd(L1)_2]$ (4-PBB, IC_{50} = 24.54 ± 0.02 μM). The two 4-Phenylbutyric acid-containing $[Cd(L1)_2]$ (4-PB1 = 40.35 ± 0.02 μM) appeared to be the least active member of the metal complexes. The increased planar surface afforded by the connected heterocyclic moieties for stacking contact with the pathogen's DNA, which results in DNA damage, may be the cause of these compounds' powerful nature, in addition to a variety of structural variables important for anti-pathogen activity. The suppression of the pathogen's active enzymes is another potential cause of activity. The active complexes may interact with the enzyme in different ways, changing its mechanism and ultimately deactivating it [51, 52]. The most effective synthesized complex, 4-PBD, killed the promastigotes even at low concentrations.

4. CONCLUSIONS

Here, Cd(II) complexes were synthesized using bioactive moieties such as nitrogen heterocycles and 4-phenylbutyric acid. The synthesis was carried out with consideration for their potential application as drugs that can target DNA. The 4-phenylbutyric acid in combination with the structural and electronic properties of 2,2′-bipyridine, 1,10-phenanthroline, and 2,9-dimethyl-1,10-phenanthroline successfully adjusted the geometric environment surrounding the Cd(II) core. The bidentate coordination of 4-phenylbutyric acid is evident by the FT-IR data. The proton and carbon of the compound under investigation are clearly responsible for the resonance signal seen in the ^{1}H and ^{13}C spectra. The compounds were found to interact with DNA by intercalation, groove binding, and mixed modes of interaction following a spontaneous process, as indicated by the -ve values of ΔG. The antileishmanial activity against *L. tropica* promastigote was assessed *in vitro* for the ligand and its derived complexes. The results imply that they could be explored further to be used as an effective drug candidate against leishmaniasis. According to the results, this type of structural design compound could be very helpful in the search and finding for new, effective treatments for DNA-related disorders.

5. ACKNOWLEDGEMENT

S.A. is grateful to the Pakistan Academy of Sciences and Quaid-i-Azam University, Islamabad for the financial assistance.

6. ETHICAL STATEMENT

In this work no human or animal subjects are involved; therefore, ethical approval was not required.

7. DECLARATION OF COMPETING INTEREST

The authors have no conflict of interest.

8. AUTHORSHIP CONTRIBUTION STATEMENT

Aneea Sharif**:** Investigation, writing original draft, review & editing. Saba Naz: Data interpretation, reviewing, editing, and overall refinement of the

manuscript**.** Saqib Ali: Conceptualization, Supervision, Project administration, Funding acquisition. Ali Haider: Methodology, Validation, Resources, review & editing. Sammar Yousuf: Antileishmanial study and its data interpretation. Mehboob ur Rehman: Software handling, formal analysis, and data curation.

9. REFERENCES

1. M. El-SayedAzab. Leishmaniasis. In: *Textbook of Parasitic Zoonoses*. S.C. Parija, and A. Chaudhury (Eds.). *Springer Nature Singapore, Singapore* pp. 107–124 (2022). https://doi.org/10.1007/978-981-16-7204-0_11
2. D. Dourado, T.S. Medeiros, É. do Nascimento Alencar, E.M. Sales, and F.R. Formiga. Curcumin-loaded nanostructured systems for treatment of leishmaniasis: a review. *Beilstein Journal of Nanotechnology* 15(1): 37-50 (2024). https://doi.org/10.3762/bjnano.15.4
3. M. Tufail and C. Wu. Retraction Note: Exploring the Burden of Cancer in Pakistan: an analysis of 2019 Data. *Journal of Epidemiology and Global Health* 15(1): 127 (2025). https://doi.org/10.1007/s44197-023-00104-5
4. K.J. Franz and N. Metzler-Nolte. Introduction: metals in medicine. *Chemical Reviews* 119(2): 727-729 (2019). https://doi.org/10.1021/acs.chemrev.8b00685
5. Z. Yin, Y. Wang, L.R. Whittell, S. Jergic, M. Liu, E. Harry, N.E. Dixon, M.J. Kelso, J.L. Beck, and A.J. Oakley. DNA replication is the target for the antibacterial effects of nonsteroidal anti-inflammatory drugs. *Chemistry & Biology* 21(4): 481-487 (2014). https://doi.org/10.1016/j.chembiol.2014.02.009
6. S. Bindu, S. Mazumder, and U. Bandyopadhyay. Non-steroidal anti-inflammatory drugs (NSAIDs) and organ damage: A current perspective. *Biochemical Pharmacology* 180: 114147 (2020). https://doi.org/10.1016/j.bcp.2020.114147
7. A.C. Santos, L.P. Monteiro, A.C. Gomes, F. Martel, T.M. Santos, and B.J.L. Ferreira. NSAID-based coordination compounds for biomedical applications: recent advances and developments. *International Journal of Molecular Sciences* 23(5): 2855 (2022). https://doi.org/10.3390/ijms23052855
8. S. Naz, N. Uddin, S. Rahim, N. Muhammad, M. Bibi, S. Yousuf, K.S. Munawar, K. Shahid, A. Haider, and S. Ali. 4-Phenylbutyric acid based homo-heteroleptic Zn (II) carboxylates: Synthesis, structural elucidation, DNA interaction through spectroscopic and computational methods as well as ALP inhibition study. *Journal of Molecular Liquids* 356: 119031 (2022). https://doi.org/10.1016/j.molliq.2022.119017
9. Z.M. Ziaie and M. Mokhtary. A Theoretical Investigation of Heterocycles with N–O Bonds Understanding the Biological Effects and Theoretical Studies: From Theory to Applicatio. *Journal of Chemical Reviews* 7(2): 166-190 (2025). https://doi.org/10.48309/jcr.2025.503047.1411
10. G. Raymoni and H.A. Ali. Synthesis, structures and various biological applications of new Zn (II) complexes having different coordination modes controlled by the drug furosemide in presence of bioactive nitrogen based ligands. *Applied Organometallic Chemistry* 33(1): e4680 (2019). https://doi.org/10.1002/aoc.4680
11. M.S. Islas, J.J.M. Medina, O.E. Piro, G.A. Echeverría, E.G. Ferrer, and P.A. Williams. Comparisons of the spectroscopic and microbiological activities among coumarin-3-carboxylate, o-phenanthroline and zinc (II) complexes. *Spectrochimica Acta Part A: Molecular and Biomolecular Spectroscopy* 198: 212-221 (2018). https://doi.org/10.1016/j.saa.2018.03.003
12. M. Borsari. Cadmium: coordination chemistry. *Encyclopedia of Inorganic and Bioinorganic Chemistry*: 1-16 (2011). https://doi.org/10.1002/9781119951438.eibc2261
13. G. Gobe and D. Crane. Mitochondria, reactive oxygen species and cadmium toxicity in the kidney. T*oxicology Letters* 198(1): 49-55 (2010). https://doi.org/10.1016/j.toxlet.2010.04.013
14. B.A. Rzigalinski and J.S. Strobl. Cadmium-containing nanoparticles: perspectives on pharmacology and toxicology of quantum dots. *Toxicology and Applied Pharmacology* 238(3): 280-288 (2009). https://doi.org/10.1016/j.taap.2009.04.010
15. H. Bibi, A. Shamim, S. Naz, M.H. Bhatti, M. ur Rehman, A. Haider, and S. Ali. Cd (II) Derivatives of Substituted Phenylacetic Acids, Synthesis, Spectroscopic Characterization and Binding Studies with DNA. *Proceedings of the Pakistan Academy of Sciences: A. Physical and Computational Sciences* 62(4): 337-347 (2025). https://doi.org/10.53560/PPASA(62-4)704
16. G. V. Scaeteanu, C. Maxim, M. Badea and R. Olar. An overview of various applications of cadmium carboxylate coordination polymers, *Molecules* 29(16): 3874 (2024) 3874. https://doi.org/10.3390/molecules29163874

17. N. Gogoleva, M. Shmelev, M. Kiskin, A. Starikov, A. Sidorov, I. Eremenko, Isomerization of Binuclear Cadmium Carboxylate Complexes $[Cd_2L_2(O_2CR)_4]$. *Russian Journal of Coordination Chemistry* 47(4):261-271 (2021). https://doi.org/10.1134/S1070328421040035
18. Y. Lin, X. Zhang, W. Chen, W. Shi, P. Cheng, Three cadmium coordination polymers with carboxylate and pyridine mixed ligands: luminescent sensors for FeIII and CrVI ions in an aqueous medium. *Inorganic Chemistry* 56(19): 11768-11778 (2017) . https://doi.org/10.1021/acs.inorgchem.7b01790
19. L. Qadeer, S. Ali, A. Haider, N. Uddin, K.S. Munawar, M. Ashfaq, M.N. Tahir, and M.U. Rehman. Synthesis, spectral elucidation and DNA binding studies of cadmium(II) carboxylates with nitrogen donor heteroligands. *Inorganic Chemistry Communications* 168: 112894 (2024). https://doi.org/10.1016/j.inoche.2024.112894
20. S. Naz, M. Sirajuddin, I. Hussain, A. Haider, A. Nadhman, A. Gul, S. Faisal, S. Ullah, S. Yousuf, and S. Ali. 2-Phenylbutyric acid based organotin (IV) carboxylates: synthesis, spectroscopic characterization, antibacterial action against plant pathogens and in vitro hemolysis. *Journal of Molecular Structure* 1203: 127378 (2020). https://doi.org/10.1016/j.molstruc.2019.127378
21. S. Naz, S. Ullah, U. Iqbal, S. Yousuf, S. Rahim, N. Muhammad, R. Fatima, I.U. Haq, A. Haider, and S. Ali. Homo-and heteroleptic 3-methylbenzoates of zinc (II) ion based on N-donor heterocycles: structure, DNA binding and pharmacological evaluation. *Journal of Molecular Liquids* 368: 120792 (2022). https://doi.org/10.1016/j.molliq.2022.120792
22. M. Zubair, M. Sirajuddin, K. Ullah, A. Haider, F. Perveen, I. Hussain, S. Ali, and M.N. Tahir. Synthesis, structural peculiarities, theoretical study and biological evaluation of newly designed O-Vanillin based azomethines. *Journal of Molecular Structure* 1205: 127574 (2020). https://doi.org/10.1016/j.molstruc.2019.127574
23. M.I. Choudhary, S. Yousuf, S.A.A. Shah, and S. Ahmed. Biotransformation of physalin H and leishmanicidal activity of its transformed products. *Chemical and Pharmaceutical Bulletin* 54(7): 927-930 (2006). https://doi.org/10.1248/cpb.54.927
24. P. Ebrahimisadr, F. Ghaffarifar, and Z.M. Hassan. In-vitro evaluation of antileishmanial activity and toxicity of artemether with focus on its apoptotic effect. *Iranian Journal of Pharmaceutical Research* 12(4): 903 (2013). https://doi.org/10.22037/ijpr.2013.1406
25. A. Sarfraz, S. Naz, A. Haider, K.S. Munawar, R. Fatima, S. Yousuf, M.N. Tahir, Y. Wasti, I.U. Haq, and S. Ali. Synthesis, Characterization, and in vitro pharmacological evaluation of Zinc (II) complexes of cycloalkanes and bioactive nitrogen donor heterocycles. *Journal of Molecular Liquids* 418: 126713 (2025). https://doi.org/10.1016/j.molliq.2024.126713
26. K.I. Hadjiivanov, D.A. Panayotov, M.Y. Mihaylov, E.Z. Ivanova, K.K. Chakarova, S.M. Andonova, and N.L. Drenchev. Power of infrared and Raman spectroscopies to characterize metal-organic frameworks and investigate their interaction with guest molecules. *Chemical Reviews* 121(3): 1286-1424 (2020). https://doi.org/10.1021/acs.chemrev.0c00487
27. P.N. Nelson and R.A. Taylor. Theories and experimental investigations of the structural and thermotropic mesomorphic phase behaviors of metal carboxylates. *Applied Petrochemical Research* 4(3): 253-285 (2014). https://doi.org/10.1007/s13203-014-0044-3
28. J. Kalembkiewicz, M. Kosińska, and L. Zapała. Complexes of aminobenzoic acids: a comprehensive review concerning synthesis, physical chemistry, structure and application. *Coordination Chemistry Reviews* 348: 25-53 (2017). https://doi.org/10.1016/j.ccr.2017.07.004
29. G. Deacon and R. Phillips. Relationships between the carbon-oxygen stretching frequencies of carboxylato complexes and the type of carboxylate coordination. *Coordination Chemistry Reviews* 33(3): 227-250 (1980). https://doi.org/10.1016/S0010-8545(00)80455-5
30. V.P. Singh, S. Singh, D.P. Singh, K. Tiwari, and M. Mishra. Synthesis, spectroscopic (electronic, IR, NMR and ESR) and theoretical studies of transition metal complexes with some unsymmetrical Schiff bases. *Journal of Molecular Structure* 1058: 71-78 (2014). https://doi.org/10.1016/j.molstruc.2013.10.046
31. K. Ullah, S. Ali, A. Haider, S. Naz, S. Yousuf, K.S. Munawar, M.S. Jan, R. Zafar, and R. Kumar. Investigation of pivalic acid-derived organotin (IV) carboxylates: Synthesis, structural insights, interaction with biomolecules, and computational studies. *Journal of Molecular Structure* 1322: 140444 (2025). https://doi.org/10.1016/j.molstruc.2024.140444
32. N. Muhammad, M. Ikram, S. Rehman, M. Ibrahim, Viola, and C. Schulzke. Structural, thermal kinetics and thermodynamics study of new mixed ligand

zinc complexes. *Journal of Thermal Analysis and Calorimetry* 128(1): 627-637 (2017). https://doi.org/10.1007/s10973-016-5842-7

33. L.Q. Chai, Q. Hu, K.Y. Zhang, L. Zhou, and J.J. Huang. Synthesis, structural characterization, spectroscopic, and DFT studies of two penta-coordinated zinc (II) complexes containing quinazoline and 1, 10-phenanthroline as mixed ligands. *Journal of Luminescence* 203: 234-246 (2018). https://doi.org/10.1016/j.jlumin.2018.06.058
34. M. Tahir, M. Sirajuddin, M. Zubair, A. Haider, A. Nadman, S. Ali, F. Perveen, H.B. Tanveer, and M.N. Tahir. Designing, spectroscopic and structural characterization and evaluation of biological potential as well as molecular docking studies of Zn (II)-based metallo-pharmaceuticals. *Journal of the Iranian Chemical Society* 18(7): 1689-1702 (2021). https://doi.org/10.1007/s13738-020-02142-3
35. S. Aslam, A.A. Isab, M.A. Alotaibi, M. Saleem, M. Monim-ul-Mehboob, S. Ahmad, I. Georgieva, and N. Trendafilova. Synthesis, spectroscopic characterization, DFT calculations and antimicrobial properties of silver (I) complexes of 2, 2′-bipyridine and 1, 10-phenanthroline. *Polyhedron* 115: 212-218 (2016). https://doi.org/10.1016/j.poly.2016.04.047
36. A.S. Gaballa, C. Wagner, S.M. Teleb, E.-M. Nour, M. Elmosallamy, G.N. Kaluđerović, H. Schmidt, and D. Steinborn. Preparation, spectroscopic and structural studies on charge-transfer complexes of 2, 9-dimethyl-1, 10-phenanthroline with some electron acceptors. *Journal of Molecular structure* 876(1-3): 301-307 (2008). https://doi.org/10.1016/j.molstruc.2007.07.003
37. R. Castro, J.A. Garcia-Vazquez, J. Romero, A. Sousa, C.A. McAuliffe, and R. Pritchard. Electrochemical synthesis of benzothiazole-2-thionato complexes of nickel (II), Zinc (II) and cadmium(II): the crystal structure of 2, 2′-bipyridine bis (benzothiazole-2-thionato) zinc (II). *Polyhedron* 12(18): 2241-2247 (1993). https://doi.org/10.1016/S0277-5387(00)88263-7
38. R. Kumar, P. Bhargava, and A. Dvivedi. Synthesis and characterization of a new cadmium complex, cadmium [(1, 10-phenanthroline) (8-hydroxyquinoline)] Cd (Phen). *Procedia Materials Science* 10: 37-43 (2015). https://doi.org/10.1016/j.mspro.2015.06.023
39. S. Ullah, M. Sirajuddin, Z. Ullah, A. Mushtaq, S. Naz, M. Zubair, A. Haider, S. Ali, M. Kubicki, and T.A. Wani. Synthesis, structural elucidation and pharmacological applications of Cu (II) heteroleptic carboxylates. *Pharmaceuticals* 16(5): 693 (2023). https://doi.org/10.3390/ph16050693
40. R. Loganathan, S. Ramakrishnan, M. Ganeshpandian, N.S. Bhuvanesh, M. Palaniandavar, A. Riyasdeen, and M.A. Akbarsha. Mixed ligand copper (II) dicarboxylate complexes: the role of co-ligand hydrophobicity in DNA binding, double-strand DNA cleavage, protein binding and cytotoxicity. *Dalton Transactions* 44(22): 10210-10227 (2015). https://doi.org/10.1039/C4DT03879G
41. M. Mishra, K. Tiwari, S. Shukla, R. Mishra, and V.P. Singh. Synthesis, structural investigation, DNA and protein binding study of some 3d-metal complexes with N′-(phenyl-pyridin-2-yl-methylene)-thiophene-2-carboxylic acid hydrazide. *Spectrochimica Acta Part A: Molecular and Biomolecular Spectroscopy* 132: 452-464 (2014). https://doi.org/10.1016/j.saa.2014.05.007
42. T. Yasmeen, S. Naz, F. Younas, S. Ali, Z. Rashid, A. Haider, M. Sirajuddin, B.S. Bassil, U. Kortz, and T.A. Wani. Heteroleptic tri-and di-organotin (IV) carboxylates: Synthesis, characterization and anticancer evaluation. *Journal of Molecular Structure* 1323: 140742 (2025). https://doi.org/10.1016/j.saa.2014.05.007
43. R. Hajian, P. Hossaini, Z. Mehrayin, P.M. Woi, and N. Shams. DNA-binding studies of valrubicin as a chemotherapy drug using spectroscopy and electrochemical techniques. *Journal of Pharmaceutical Analysis* 7(3): 176-180 (2017). https://doi.org/10.1016/j.jpha.2017.01.003
44. Y. Li, Z.-Y. Yang, and M.-F. Wang. Synthesis, characterization, DNA binding properties, fluorescence studies and antioxidant activity of transition metal complexes with hesperetin-2-hydroxy benzoyl hydrazone. *Journal of Fluorescence* 20(4): 891-905 (2010). https://doi.org/10.1007/s10895-010-0635-z
45. A. Tarushi, G. Psomas, C.P. Raptopoulou, and D.P. Kessissoglou. Zinc complexes of the antibacterial drug oxolinic acid: structure and DNA-binding properties. *Journal of Inorganic Biochemistry* 103(6): 898-905 (2009). https://doi.org/10.1016/j.jinorgbio.2009.03.007
46. G. Psomas. Mononuclear metal complexes with ciprofloxacin: Synthesis, characterization and DNA-binding properties. *Journal of Inorganic Biochemistry* 102(9): 1798-1811 (2008). https://doi.org/10.1016/j.jinorgbio.2008.05.012
47. S.U. Rehman, T. Sarwar, M.A. Husain, H.M. Ishqi, and M. Tabish. Studying non-covalent drug–DNA interactions. *Archives of Biochemistry and Biophysics* 576: 49-60 (2015). https://doi.

org/10.1016/j.abb.2015.03.024

48. B. Amritha and S. Vasudevan. Synthesis, characterisation, and DNA interaction studies of novel Cu (II), Ni (II), and Co (II) mono and bisligand complexes of N-(1, 10-phenanthrolin-5-yl) acridine-9-carboxamide. *Chemical Papers* 74(6): 1979-1996 (2020). https://doi.org/10.1007/s11696-019-01041-z
49. Y.J. Liu, X.Y. Guan, X.Y. Wei, L.X. He, W.J. Mei, and J.H. Yao. Ruthenium (II) complexes containing 2, 9-dimethyl-1, 10-phenanthroline and 4, 4′-dimethyl-2, 2′-bipyridine as ancillary ligands: synthesis, characterization and DNA-binding. *Transition Metal Chemistry* 33(3): 289-294 (2008). https://doi.org/10.1007/s11243-007-9042-y
50. S. Naz, N. Uddin, K. Ullah, A. Haider, A. Gul, S. Faisal, A. Nadhman, M. Bibi, S. Yousuf, and S. Ali. Homo-and heteroleptic Zinc (II) carboxylates: Synthesis, structural characterization, and assessment of their biological significance in in vitro models. *Inorganica Chimica Acta* 511: 119849 (2020). https://doi.org/10.1016/j.ica.2020.119849
51. G. Colotti, A. Ilari, A. Fiorillo, P. Baiocco, M.A. Cinellu, L. Maiore, F. Scaletti, C. Gabbiani, and L. Messori. Metal-based compounds as prospective antileishmanial agents: inhibition of trypanothione reductase by selected gold complexes. *ChemMedChem* 8(10): 1634-1637 (2013). https://doi.org/10.1002/cmdc.201300276
52. Y.C. Ong, L. Kedzierski, and P.C. Andrews. Do bismuth complexes hold promise as antileishmanial drugs? *Future Medicinal Chemistry* 10(14): 1721-1733 (2018). https://doi.org/10.4155/fmc-2017-0287